

## **Electronic Supplementary Information**

# **Bio-Bar-Code Functionalized Magnetic Nanoparticle Label for Ultrasensitive Flow Injection Chemiluminescence Detection of DNA Hybridization**

Sai Bi, Hong Zhou, Shusheng Zhang\*

*Key Laboratory of Eco-chemical Engineering, Ministry of Education, College of Chemistry and  
Molecular Engineering, Qingdao University of Science and Technology, Qingdao 266042, China*

## EXPERIMENTAL SECTION

**Apparatus.** The CL measurements were performed with a FI-CL instrument (MPI-F, Remex Analytical Instrument Co. Ltd., Xi'an, China), including a model IFIS-D flow injection system, a model RFL-1 luminometer, and a computer. The kinetics of CL signals after adding quenchers to luminol-H<sub>2</sub>O<sub>2</sub>-Fe<sup>3+</sup> system were obtained by a BPCL ultraweak luminescence analyzer (Institute of Biophysics Academic Sinica, Beijing, China). The electrochemical impedance spectroscopy (EIS) were carried out on a CHI 660C electrochemical working station (CH Instrument Co.) with a three-electrode system that consisted of a platinum wire as auxiliary electrode, an Ag/AgCl electrode as reference electrode, and Au disk electrode as working electrode. Transmission electron microscopy (TEM) images were acquired on a JEM-2000EX/ASID2 (HITACHI, Japan). A CARY 500 Scan UV/Vis-NIR spectrophotometer (Varian, USA) was used to record the UV-vis absorption spectra. Carboxyl groups modified magnetic nanoparticles (~ 500 nm, 10 mg mL<sup>-1</sup>) and magnetic rack were obtained from BaseLine ChromTech Research Centre (Tianjin, China).

**Reagents.** 1-Ethyl-3-(3-dimethylaminopropyl)-carbodiimide hydrochloride (EDC) and imidazole were purchased from Sigma. 6-Mercapto-1-hexanol (MCH) was obtained from Fluka (Switzerland). H<sub>2</sub>O<sub>2</sub> with analytical grade was from Shanghai Chemical Reagent Company (Shanghai, China). Superoxide Dismutase (SOD) was obtained from Worthington Biochemical Corporation, and mannitol and methanol from Sinopharm Chemical Reagent (China). A luminol (standard powder, Sigma-Aldrich) stock solution ( $1.0 \times 10^{-2}$  M) was prepared by dissolution in 0.1 M NaOH and further stored in dark. The stock solution was consecutively diluted with 0.1 M Na<sub>2</sub>B<sub>4</sub>O<sub>7</sub>-NaOH in order to obtain the proper solution used for CL determination. Ferriammonium sulfate was ordered from Tianjin Yaohua Chemical Reagent Co., Ltd. (China). The 0.1 M PBS buffer (pH 7.4), 0.1 M imidazol-HCl buffer (pH 7.0), 0.025 M tris-HCl buffer (pH 8.2) and 0.1 M Na<sub>2</sub>B<sub>4</sub>O<sub>7</sub>-NaOH buffer (pH 10.0) were prepared according to the standard methods. All the DNA sequences were synthesized and purified by SBS Genetech Co. Ltd. (China), and the sequences of this work are listed in [Table S1](#).

Deionized and doubly distilled water was used throughout the experiments. All the chemicals employed were of analytical reagent grade and were used without further purification.

**Table S1. DNA Sequence Used in This Work**

oligonucleotides name	sequences <sup>a</sup>	description
capture DNA (cDNA)	5'-TGG AAA ATC TCT AGC AGT CGT-(CH <sub>2</sub> ) <sub>6</sub> -SH-3'	thiolated capture DNA immobilized on Au electrode
target DNA (tDNA)	5'-ACT GCT AGA GAT TTT CCA CAC TGA CTA AAA GGG TCT GAG GGA-3'	complementary to cDNA and pDNA
probe DNA (pDNA)	5'-NH <sub>2</sub> -(CH <sub>2</sub> ) <sub>6</sub> -ATG TCC CTC AGA CCC TTT-3'	amino group modified probe DNA coated on MNPs and complementary to tDNA
fluorescein labeled cDNA	5'-FAM-TGG AAA ATC TCT AGC AGT CGT-(CH <sub>2</sub> ) <sub>6</sub> -SH-3'	to determine the surface coverage of alkanethiol-functionalized cDNA adsorbed onto Au electrode
bio-bar-code DNA (bbcDNA)	5'-CCA ACC ACA CCA ACC-NH <sub>2</sub> -3'	amino group modified probe DNA coated on MNPs and noncomplementary to tDNA
fluorescein labeled bbcDNA (F-bbcDNA)	5'-F-CCA ACC ACA CCA ACC-NH <sub>2</sub> -3'	amino group modified probe DNA with 5' end labeled fluorescein and noncomplementary to tDNA
two-base mismatch DNA	5'-ACT GCT ACA GAT TTT CCA CAC TGA CTA AAA <u>G</u> <u>C</u> G TCT <u>G</u> <u>T</u> G GGA-3'	These two sequences are used to determination the selectivity of the proposed assay
noncomplementary DNA (noncDNA)	5'-ACT GCT AGA GAT TTT CCA CAC TGA CTA AAA GGG TCT GAG GGA-3'	

<sup>a</sup> The mismatched bases in DNA sequences are marked out with italic and underlined.

**Preparation of bbc-p-DNA-MNPs.** The bbc-p-DNA-MNPs were prepared according to the reference with a slight modification. Briefly, 50  $\mu$ L suspension of carboxylated MNPs was placed in a 1.5 mL Eppendorf tube (EP tube) and separated from the solution on a magnetic rack. After washing three times with 200  $\mu$ L of 0.1 M imidazol-HCl buffer (pH 7.0), a 0.1 M imidazol-HCl buffer (100  $\mu$ L) and a 0.8 M EDC (100 $\mu$ L) were added to the EP tube and the mixture was incubated at 37°C for 30 min to activate the carboxylate groups on the MNPs, followed by washing three times with 200 $\mu$ L of 0.1 M PBS buffer and resuspending to a final volume of 200  $\mu$ L. And then a mixture of  $1.2 \times 10^{-10}$  mol of pDNA and  $1.2 \times 10^{-9}$  mol of bbcDNA was added to the above freshly activated MNPs, and incubated at 37°C overnight. Finally, the resulting bbc-p-MNPs were washed with 200 $\mu$ L of 0.1 M PBS buffer for three times, and resuspended in 200  $\mu$ L PBS buffer and stored at 4 °C for further use.

**Preparation of CL Biosensor.** The procedure of the fabrication of CL biosensor and the principle of MNPs-based CL detection of DNA hybridization are illustrated in [Scheme 1](#) in the manuscript. Briefly, Au electrodes (2 mm in diameter, CH Instruments Inc.) were first cleaned in piranha

solution (70% H<sub>2</sub>SO<sub>4</sub>/30% H<sub>2</sub>O<sub>2</sub>) (WARNING: piranha reacts violently with organics), and rinsed with deionized and doubly distilled water. Subsequently, the electrodes were polished with alumina slurries (1, 0.3, 0.05 μm). After sonicated in deionized and doubly distilled water, the electrodes were dried with nitrogen gas to remove any remaining impurities.

After drying with nitrogen, electrodes were immersed in 1 mL of 0.1 M PBS buffer containing 1.0 × 10<sup>-7</sup> M thiolated cDNA at room temperature overnight, followed by immersing in 1 mM MCH for 1.5 h to block the uncovered Au electrode surface, and further to avoid consequent nonspecific adsorption in the following hybridization procedures. The sandwich-type hybridization was carried out as the following two steps: First, the cDNA-modified Au electrodes were incubated with appropriate concentrations tDNA solutions in 0.1 M PBS buffer for 1.5 h at 37 °C. And then, the modified tDNA/cDNA/Au electrodes were taken out and immersed into 0.1 M PBS buffer containing bbc-pDNA-MNPs for 1 h at 37°C to perform the sandwich-type hybridization with tDNA. After each hybridization procedure, the electrodes were rinsed with 0.1 M PBS buffer to remove nonspecifically adsorbed sequences.

**FI-CL detection.** First, Au electrode modified with sandwich-type hybrids labeled with MNPs was immersed into a colorimetric tube containing 200 μL of 0.4 M nitric acid solution for 30 min. The MNPs which had been anchored on the hybrids were dissolved completely. And then, the volume of the solution was adjusted to 4 mL with deionized and doubly distilled water, and the pH of the above solution was adjusted to 4.0 through 0.1 M nitric acid for FI-CL detection. In the following FI-CL detection, 5.0 × 10<sup>-4</sup> M luminol in pH 10.0, 0.1 M Na<sub>2</sub>B<sub>4</sub>O<sub>7</sub>-NaOH buffer solution was first mixed with 2.0 × 10<sup>-3</sup> M H<sub>2</sub>O<sub>2</sub> (both pumped by pump 1), and then reacted with metal ions (pumped by pump 2) in the flow cell to produce CL signal.

#### **Optimization of luminol-H<sub>2</sub>O<sub>2</sub>-Fe<sup>3+</sup> CL system**

#### **Effect of flow-injection mode for luminol-H<sub>2</sub>O<sub>2</sub>-Fe<sup>3+</sup>.**

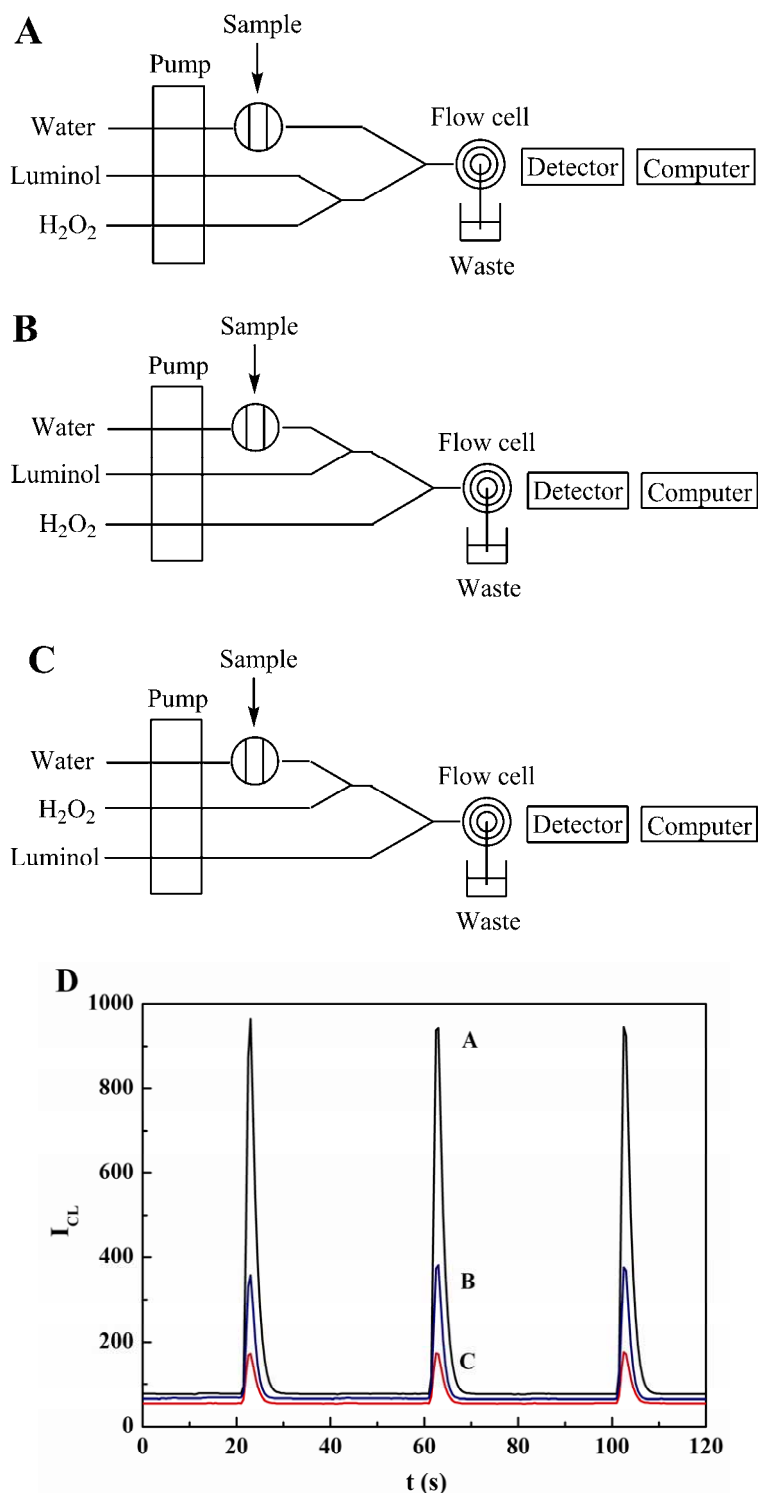


Fig. S1. (A-C) The schematic diagram of different modes for FI-CL detection system for the determination of  $Fe^{3+}$ . (D) The kinetic curves of luminol CL reactions by three different FI-CL modes. The annotation A-C in D are corresponding to the FI modes of A-C.

From Fig. S1, mode A was the most effective FI mode for luminol-H<sub>2</sub>O<sub>2</sub>- $Fe^{3+}$  CL system, in which luminol solution was first mixed with H<sub>2</sub>O<sub>2</sub> and then with ferric ions. And we adopted mode A for the following experiments.

### Effect of the high potential of the photomultiplier tube.

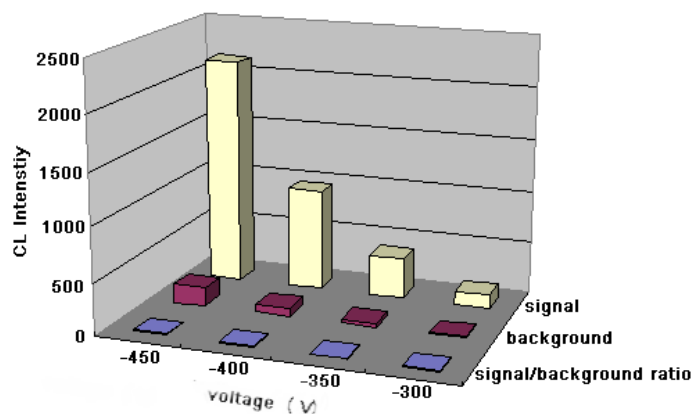


Fig. S2. The effect of the high potential of the photomultiplier tube.

Considering both of the CL intensity and the signal/background ratio, the high potential of the photomultiplier tube was set as -400 V for the following experiments..

### Effect of buffer solutions and pH values.

The effect of buffer solutions, including  $\text{H}_3\text{BO}_3\text{-NaOH}$ ,  $\text{NaHCO}_3\text{-Na}_2\text{CO}_3$ ,  $\text{Na}_2\text{HPO}_4\text{-NaOH}$ ,  $\text{NaHCO}_3\text{-NaOH}$ ,  $\text{Na}_2\text{B}_4\text{O}_7\text{-NaOH}$  and  $\text{Na}_2\text{B}_4\text{O}_7\text{-Na}_2\text{CO}_3$  in the pH range from 9.5 to 12.0 was studied. As shown in Fig. S3A, the CL reaction was most active upon using luminol prepared by 0.1 M the  $\text{Na}_2\text{B}_4\text{O}_7\text{-NaOH}$  buffer solution, and pH 10.0 was tentatively adopted for further experiment.

### Effect of luminol and $\text{H}_2\text{O}_2$ concentrations.

The effects of luminol and  $\text{H}_2\text{O}_2$  concentrations were investigated. It was found that both the CL intensity and signal/background ratio increased with an increase in luminol concentration in the range from  $1.0 \times 10^{-4}$  to  $5.0 \times 10^{-4}$  mol/L, and decreased over the concentration of  $5.0 \times 10^{-4}$  mol/L. As shown in Fig. S3B, the maximal CL signal/background ratio was obtained at  $5.0 \times 10^{-4}$  mol/L luminol concentration. Therefore, the luminol concentration of  $5.0 \times 10^{-4}$  mol/L was chosen as the optimal concentration.

The effect of hydrogen peroxide concentrations on the CL intensity was investigated in the range of  $2.0 \times 10^{-3}$  mol/L. As shown in Fig. S3C, the CL intensity increased with increasing  $\text{H}_2\text{O}_2$  concentration in the range of  $2.0 \times 10^{-4}$  to  $2.0 \times 10^{-3}$  mol/L, then the maximal signal occurred at  $2.0 \times 10^{-3}$  mol/L and decreased with further increase of  $\text{H}_2\text{O}_2$  concentrations.

### Effect of pH of Fe<sup>3+</sup> standard solution.

The pH value of Fe<sup>3+</sup> standard solution is another critical factor for luminol-H<sub>2</sub>O<sub>2</sub>-Fe<sup>3+</sup> CL reaction system. Through adjusting the pH values of Fe<sup>3+</sup> standard solution in the range of 3.0 to 7.0, we studied the pH effect on luminol-H<sub>2</sub>O<sub>2</sub>-Fe<sup>3+</sup> CL reaction system (Fig. S3D). The maximum CL signal/background ratio was obtained at pH of 4.0 for Fe<sup>3+</sup> standard solution.

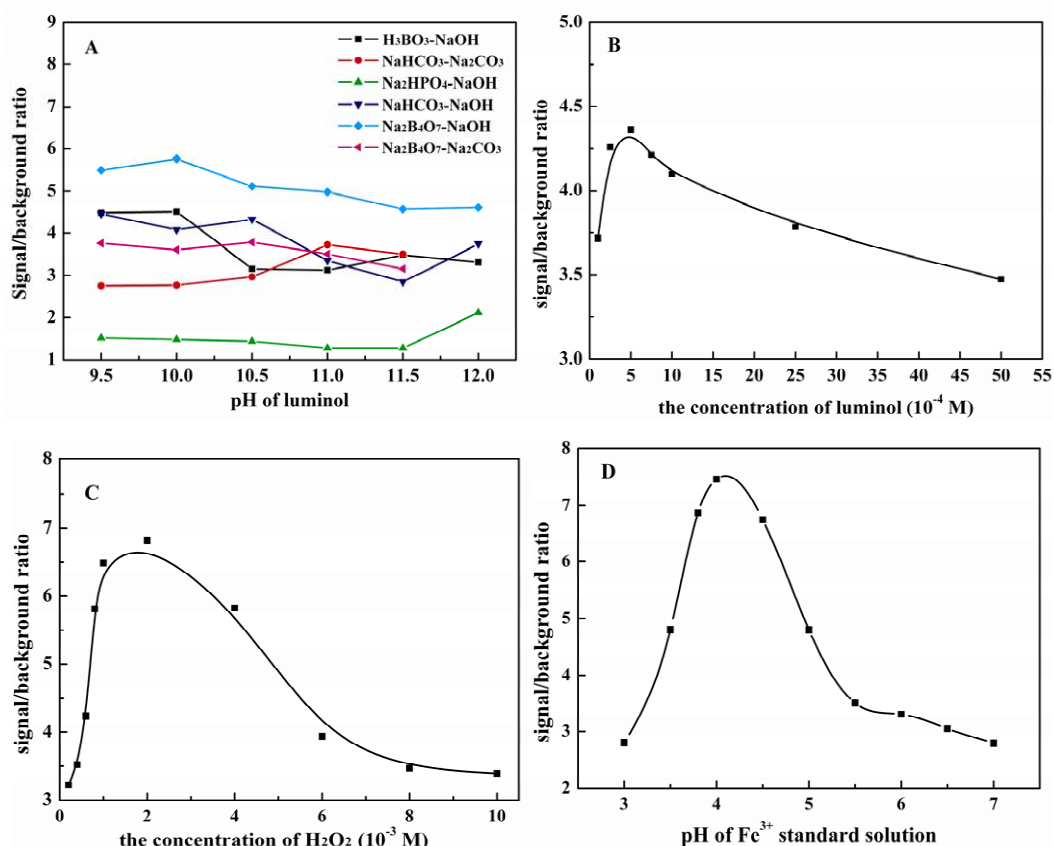


Fig. S3. Effects of the reactant conditions on the luminol-H<sub>2</sub>O<sub>2</sub>-Fe<sup>3+</sup> CL system. (A) Effects of luminol pH: 5.0 × 10<sup>-4</sup> M luminol, 1.7 × 10<sup>-3</sup> M H<sub>2</sub>O<sub>2</sub> and pH 3.8, 2.0 × 10<sup>-8</sup> g/mL Fe<sup>3+</sup> solution. (B) Effects of the concentration of luminol: pH 10.0, 0.1 M Na<sub>2</sub>B<sub>4</sub>O<sub>7</sub>-NaOH buffer solution, 1.7 × 10<sup>-3</sup> M H<sub>2</sub>O<sub>2</sub> and pH 3.8, 2.0 × 10<sup>-8</sup> g/mL Fe<sup>3+</sup> solution. (C) Effects of the concentration of H<sub>2</sub>O<sub>2</sub>: 5.0 × 10<sup>-4</sup> M luminol in pH 10.0, 0.1 M Na<sub>2</sub>B<sub>4</sub>O<sub>7</sub>-NaOH buffer solution, pH 3.8, 2.0 × 10<sup>-8</sup> g/mL Fe<sup>3+</sup> solution. (D) Effects of Fe<sup>3+</sup> solution pH: 5.0 × 10<sup>-4</sup> M luminol in pH 10.0, 0.1 M Na<sub>2</sub>B<sub>4</sub>O<sub>7</sub>-NaOH buffer solution, 2.0 × 10<sup>-3</sup> M H<sub>2</sub>O<sub>2</sub> and 2.0 × 10<sup>-8</sup> g/mL Fe<sup>3+</sup> solution.

### Effect of the concentrations of ferric ions.

The effect of concentration of ferric ions was also investigated (Fig. S4). It was found that the CL intensity increased gradually with increasing the concentration of Fe<sup>3+</sup>. The catalysed CL

intensity was found to be linear with the concentration of  $\text{Fe}^{3+}$ . As shown in Fig. S4, the nonlinear function for  $\text{Fe}^{3+}$  could be expressed as  $Y = -0.0853 X^2 + 16.0359 X + 31.4385$  (Y is the CL intensity; X is the concentration of  $\text{Fe}^{3+}$ ,  $10^{-10}$  M;  $n = 12$ ,  $R^2 = 0.9958$ ) from  $1.0 \times 10^{-10}$  to  $1.0 \times 10^{-8}$  g/mL  $\text{Fe}^{3+}$ . The concentration of  $1.0 \times 10^{-10}$  to  $1.0 \times 10^{-9}$  g/mL  $\text{Fe}^{3+}$  could be expressed as the linear regression equation of  $Y = 20.6655 X + 8.4812$  (X is the concentration of ferric ion,  $10^{-10}$  g/mL; Y is the CL intensity,  $n = 7$ ,  $R = 0.9980$ ).

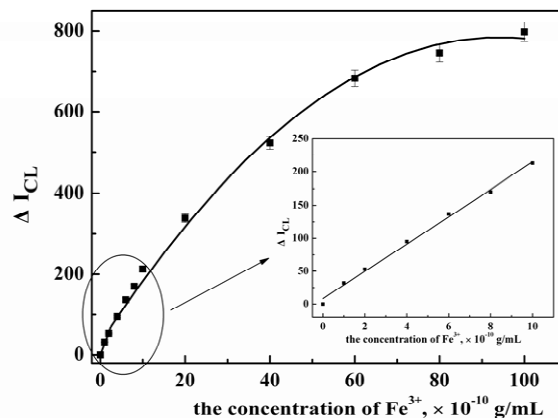


Fig. S4. CL signal calibration curve of  $\text{Fe}^{3+}$  standard solution. The concentration of luminol and  $\text{H}_2\text{O}_2$  were  $5.0 \times 10^{-4}$  M in pH 10.0  $\text{Na}_2\text{B}_4\text{O}_7\text{-NaOH}$  buffer solution and  $2.0 \times 10^{-3}$  M, respectively. The pH of  $\text{Fe}^{3+}$  standard solution was 4.0.

#### Calculation of the surface coverages of pDNA and bbcDNA on MNPs used in this study

##### Preparation of UV-vis Calibration Curve of pDNA

Standard pDNA solutions were prepared from the solution of  $1.0 \times 10^{-6}$  M pDNA with deionized and doubly distilled water. The UV-vis absorbance calibration curve of pDNA is shown in Fig. S5, the regression equation could be expressed as  $Y = 0.02047X - 0.00074$  (X is the concentration of DNA,  $10^{-7}$  M; Y is the absorbance of UV-vis,  $n = 6$ ,  $R = 0.9986$ ).

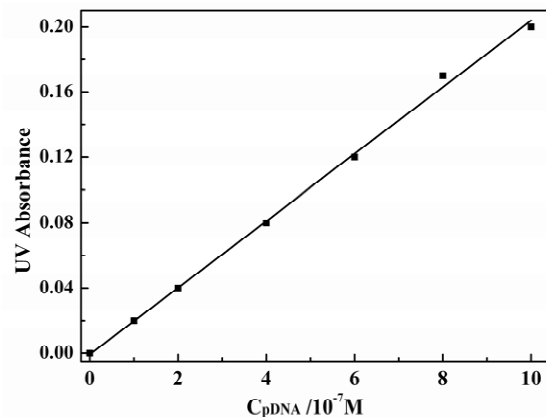


Fig. S5. UV absorbance calibration curve of pDNA solution.

### Preparation of Fluorescence Calibration Curve

Fluorescein modified bbcDNA (F-bbcDNA) was used to fluorescence detection. The fluorescence responses and calibration curve of bbcDNA probe are shown in Fig. S6, the regression equation could be expressed as  $Y = 327.23X + 33.97$  ( $X$  is the concentration of DNA,  $10^{-7}$  M;  $Y$  is the fluorescence intensity,  $n = 11$ ,  $R = 0.9998$ ).

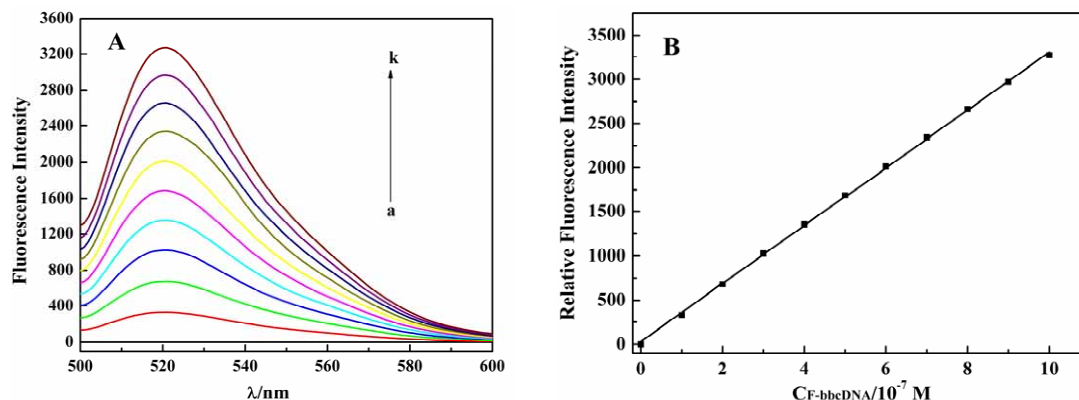


Fig. S6. (A) Fluorescence responses towards different concentration F-bbcDNA of (a) 0, (b)  $1.0 \times 10^{-7}$ , (c)  $2.0 \times 10^{-7}$ , (d)  $3.0 \times 10^{-7}$ , (e)  $4.0 \times 10^{-7}$ , (f)  $5.0 \times 10^{-7}$ , (g)  $6.0 \times 10^{-7}$ , (h)  $7.0 \times 10^{-7}$ , (i)  $8.0 \times 10^{-7}$ , (j)  $9.0 \times 10^{-7}$ , (k)  $1.0 \times 10^{-6}$  M. (B) The fluorescence calibration curve of F-bbcDNA corresponding to the fluorescence spectra of (A).

### Determination of the surface coverages of pDNA and bbcDNA on MNPs

2 mL of  $7 \times 10^{-7}$  M pDNA was added into the activated 100  $\mu$ L MNPs and incubated overnight in 37°C. Then 2 mL supernatant was taken for UV-vis absorbance detection. The number of pDNA immobilized on the MNPs can be quantitatively calculated from the absorbance difference at 260 nm between the DNA solution before and after immobilization, which is calculated as below.

UV absorbance of the supernatant before immobilization: 0.14221

Concentration of pDNA before immobilization:  $6.98 \times 10^{-7}$  M

UV absorbance of the supernatant after immobilization: 0.02406

Concentration of pDNA after immobilization:  $1.21 \times 10^{-7}$  M

Moles of total DNA immobilized on MNPs:  $(6.98 \times 10^{-7} - 1.21 \times 10^{-7}) \times 2 \times 10^{-3} = 1.15 \times 10^{-9}$  mole

180  $\mu\text{L}$  of  $7.0 \times 10^{-7}$  M pDNA and 1.8 mL of  $7 \times 10^{-7}$  M F-bbcDNA were added into the activated 100  $\mu\text{L}$  MNPs and incubated as described in Experimental Section in the manuscript. Then 2 mL supernatant was taken for fluorescence intensity detection. The number of F-bbcDNA immobilized on the MNPs can be quantitatively calculated from fluorescence intensity between the DNA solution before and after immobilization, which is calculated below.

Fluorescence intensity of the supernatant before immobilization: 2118

Concentration of F-bbcDNA before immobilization:  $6.37 \times 10^{-7}$  M

Fluorescence intensity the supernatant after immobilization: 538

Concentration of F-bbcDNA after immobilization:  $1.54 \times 10^{-7}$  M

Moles of F-bbcDNA immobilized on MBs:  $(6.37 \times 10^{-7} - 1.54 \times 10^{-7}) \times 2 \times 10^{-3} = 9.66 \times 10^{-10}$  mole

#### Calculation of moles of MNP in a given preparation

MNP diameter =  $0.75 \times 10^{-4}$  cm

MNP Volume =  $4/3\pi r^3 = 1.77 \times 10^{-12}$  cm<sup>3</sup>

Mass MNP =  $\rho_{\text{MNP}} \times V_{\text{MNP}} = 1.18 \times 1.77 \times 10^{-12} = 2.09 \times 10^{-12}$  (g / MNP)

The amount of MNP in 100  $\mu\text{L}$  of 0.01 g/mL MNP solution for the preparing

$(0.01 \times 0.1) / 2.09 \times 10^{-12} / 6.02 \times 10^{23} = 7.95 \times 10^{-16}$  moles

**Table S2 Quantitative Determination of the surface coverages of pDNAs and bbcDNAs on MNPs**

MNPs (mol)	total DNA (mol)	F-bbcDNA (mol)	pDNA (mol)	ratio of MNPs/ pDNA/ F-bbcDNA
$7.95 \times 10^{-16}$	$1.15 \times 10^{-9}$	$9.66 \times 10^{-10}$	$1.34 \times 10^{-10}$	$1/1.69 \times 10^5 / 1.22 \times 10^6$

#### Quantitation of surface coverage of thiolated cDNA on Au electrode

In order to determine the sufficiency of the gold surface for the experiment, a fluorescence-based method was used to determine the surface coverage of synthesized 21-mer cDNA with an alkanethiol moiety at the 3' terminal and a FAM-label at the 5' end adsorbed on Au electrode

surface (See Notes and references (12) of the new manuscript, the sequence of the FAM-alkanethiol-modified cDNA is listed in Table S2 in new ESI).

The fluorescent thiolated cDNA was assembled on the Au electrode according to the method of “Preparation of CL Biosensor” in ESI. And then mercaptoethanol (ME) with a final concentration of 0.1 M was added to displace the surface-bound cDNA via exchange reaction with intermittent shaking for 18 h at room temperature. The displacement reaction is rapid, which is presumably due to the inability for the DNA film to block access of the ME to the gold surface, and the amount of DNA free in exchange with ME increased until ~10 h of exposure, thus we chose 18 h as the exchange reaction time between ME and FAM-alkanethiol-modified cDNA. The resulting solution containing displaced FAM-cDNA was separated from the Au electrode by removal of the electrode, and the fluorescence maximums were converted to molar concentrations of the FAM-alkanethiol-modified cDNA by interpolation from a standard linear calibration curve. The standard curve was obtained according to the method of “Preparation of Fluorescence Calibration Curve” for “Calculation of the surface coverages of pDNA and bbcDNA on MNPs used in this study” in ESI (Fig. S7). The regression equation could be expressed as  $Y = 2.67X + 0.30$  (X is the concentration of DNA,  $10^{-9}$  M; Y is the fluorescence intensity,  $n = 11$ ,  $R = 0.9988$ ). Finally, the surface coverage is calculated to be 2.9 pmol on the Au electrode surface with a diameter of 2.0 mm, that is,  $\sim 5.6 \times 10^{13}$  strands/cm<sup>2</sup> by dividing the measured DNA amounts by the area of the Au electrode.

The Au electrode used in this study with a diameter of ~2.0 mm is one of the most widely employed electrode patterns in DNA detection, and there are also some other Au electrodes and Au nanoparticles with larger area used in the immobilization of ssDNA which could achieve assembling more DNA strands calculated by the above fluorescence method. Furthermore, in the following DNA hybridization study, the amount of target DNA is below amol level due to the high sensitivity of the present work. Thus, it is reasonable that any gold surface is sufficient for the assembling DNA on the electrode surface and can be further used in DNA hybridization detection.

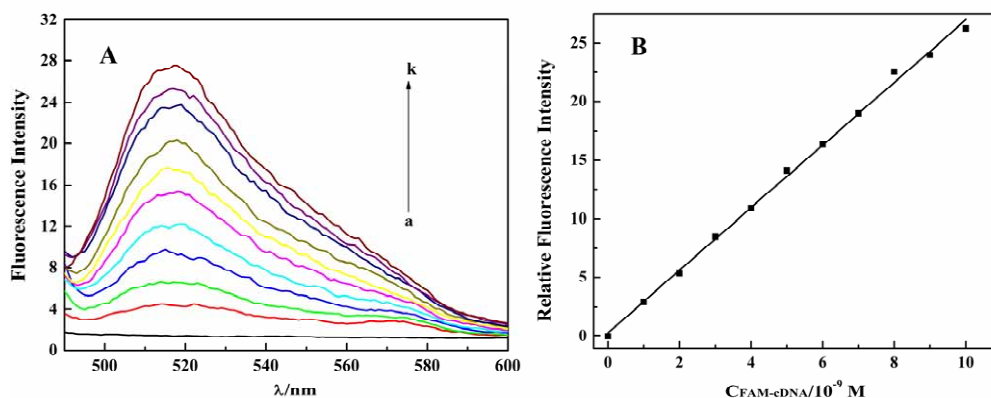


Fig. S7. (A) Fluorescence responses towards different concentration FAM-cDNA of (a) 0, (b)  $1.0 \times 10^{-9}$ , (c)  $2.0 \times 10^{-9}$ , (d)  $3.0 \times 10^{-9}$ , (e)  $4.0 \times 10^{-9}$ , (f)  $5.0 \times 10^{-9}$ , (g)  $6.0 \times 10^{-9}$ , (h)  $7.0 \times 10^{-9}$ , (i)  $8.0 \times 10^{-9}$ , (j)  $9.0 \times 10^{-9}$  M, (k)  $1.0 \times 10^{-8}$  M. (B) The fluorescence calibration curve of FAM-cDNA corresponding to the fluorescence spectra of (A).

#### The control experiment of the sensitivity of the DNA biosensor.

A control experiment was carried out to determine of the sensitivity of the DNA biosensor without using bbcDNA probe. As shown in Fig. S7A, the CL intensities of luminol- $\text{H}_2\text{O}_2\text{-Fe}^{3+}$  increased with the increase of concentration of tDNA ranging from  $1.0 \times 10^{-14}$  to  $1.0 \times 10^{-12}$  M (Fig. S7B) and started to level off afterwards. The linear range for tDNA was  $1.0 \times 10^{-14}$  to  $1.0 \times 10^{-13}$  M with the equation of  $I = 16.0853C + 3.9078$  ( $I$  is the CL intensity;  $C$  is the concentration of tDNA,  $10^{-14}$  M;  $n = 7$ ,  $R^2 = 0.9983$ ). The detection limit of 5.6 fM tDNA can be estimated using  $3\sigma$ , which was one order of magnitude higher than that obtained by employing bbcMNPs. Based on the surface coverages of pDNA and bbcDNA on MNPs (pDNA/bbcDNA = 1/7), it is suitable that the detection limit of the proposed method was 10-fold lower than that obtained by signal pDNA-MNPs as probes.

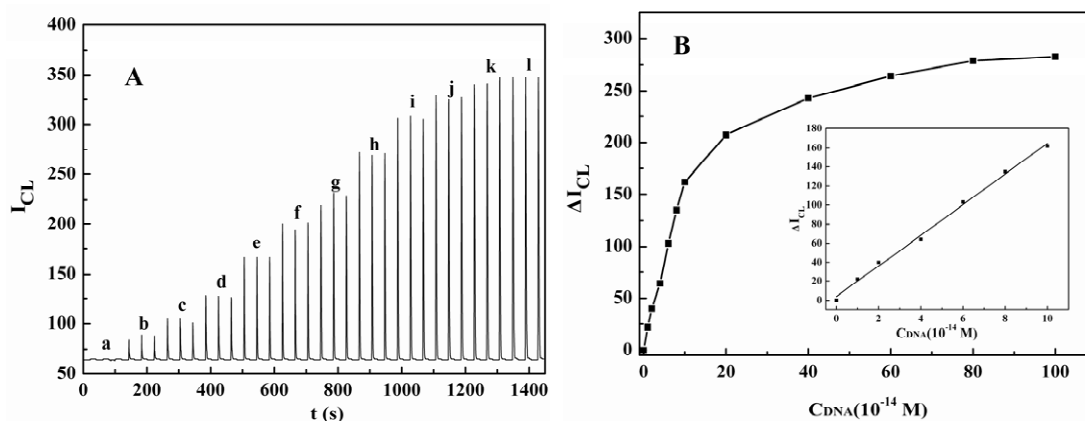


Fig. S8. (A) CL signals for  $\text{Fe}^{3+}$  dissolved from different hybrids without employing bbcDNA. The concentrations of t-DNA: (a) 0; (b)  $1.0 \times 10^{-14}$ ; (c)  $2.0 \times 10^{-14}$ ; (d)  $4.0 \times 10^{-14}$ ; (e)  $6.0 \times 10^{-14}$ ; (f)  $8.0 \times 10^{-14}$ ; (g)  $1.0 \times 10^{-13}$ ; (h)  $2.0 \times 10^{-13}$ ; (i)  $4.0 \times 10^{-13}$ ; (j)  $6.0 \times 10^{-13}$ ; (k)  $8.0 \times 10^{-13}$ ; (l)  $1.0 \times 10^{-12}$  M. (B) The calibration curve of peak height versus the concentration of tDNA from  $1.0 \times 10^{-14}$  to  $1.0 \times 10^{-12}$  M. Inset is the amplification of the linear range from  $1.0 \times 10^{-14}$  to  $1.0 \times 10^{-13}$  M for tDNA determination.

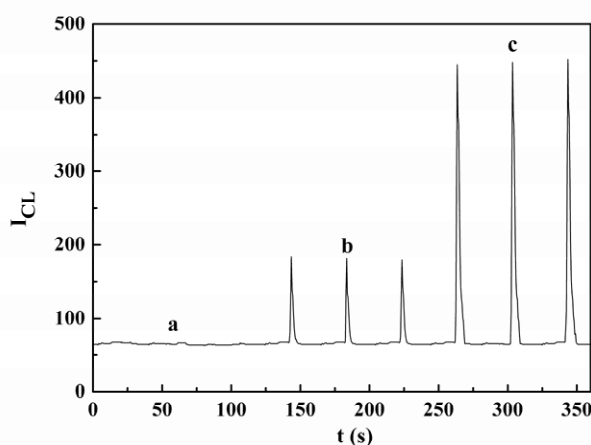


Fig. S9. FI-CL signals of luminol- $\text{H}_2\text{O}_2$  catalyzed by ferric ions dissolved from bbc-p-DNA-MNPs hybridized with different target DNA. (a) Noncomplementary sequences; (b) single-base mismatched sequences; (c) complementary sequences. All the concentrations of tDNA are  $6.0 \times 10^{-14}$  M.

**Table S3. Comparison between the Proposed CL Assay and Other Reported Techniques for the Detection of DNA Hybridization<sup>a</sup>**

format	label	techniques <sup>c</sup>	detection limit of ssDNA	no. of steps
nanoparticle and	Au nanoparticles (cross-linked) <sup>1</sup>	colorimetric	~10 nM	2
nanostructure-based	Au nanoparticles (cross-linked) <sup>2</sup>	electrochemical	100 fM	4
methods for DNA hybridization	Au NPs (non-cross-linked) <sup>3</sup>	colorimetric	60 nM	2
	Au NPs <sup>4</sup>	laser diffraction	~50 fM	4
	Au NPs <sup>5</sup>	SPR	10 pM	4
	Au NPs <sup>6</sup>	PSA	15 nM	6
	Au NPs <sup>7</sup>	chronocoulometric	10 fM	6
	Au NPs with Ag amplification <sup>8,9</sup>	Scanometric	50 fM	5
	Au NPs with Ag	Raman spectroscopy	~20 fM	5

amplification <sup>10</sup>			
Au NPs with Ag amplification <sup>11</sup>	electrical	500 fM	5
Au NPs with Ag amplification <sup>12</sup>	PSA	32 pM	7
silver NPs <sup>13</sup>	ASV	0.5 pM	4
silver NPs <sup>14</sup>	CL	5 fM	7
CuS NPs <sup>15</sup>	CL	550 fM	5
ZnS, CdS, PbS NPs <sup>16</sup>	stripping voltammetry	270 pM	5
ZnS and CdSe quantum dots <sup>17</sup>	fluorescence	2 nM	5
Liposome <sup>18</sup>	liposome-amplified electrochemical	50 fM	6
MNPs <sup>19</sup>	magnetically amplified electrochemical	0.5 fM	5
MNPs <sup>20</sup>	PSA	0.1 fM	5
Au NPs with Ag amplification <sup>21</sup>	bio-bar-code amplified scanometric	0.5 fM	8
Au and CuS NPs <sup>22</sup>	CL	4.8 fM	7
MNPs <sup>b</sup>	bio-bar-code amplified CL	0.32 fM	6

<sup>a</sup> Some were adapted from ref 22. <sup>b</sup> This method. <sup>c</sup> PSA, potentiometric stripping analysis; ASV, anodic stripping voltammetry; SPR, surface Plasmon resonance.

## Notes and references

- (1) Elghnani, R.; Storhoff, J. J.; Mucic, R. C.; Letsinger, R. L.; Mirkin, C. A. *Science* **1997**, *277*, 1078-1081.
- (2) Li, D.; Yan, Y.; Wieckowska, A.; Willner, I. *Chem. Commun.* **2007**, *34*, 3544-3546.
- (3) Sato, K.; Hosokawa, K.; Maeda, M. *J. Am. Chem. Soc.* **2003**, *125*, 8102-8103.
- (4) Bailey, R. C.; Nam, J. M.; Mirkin, C. A.; Hupp, J. T. *J. Am. Chem. Soc.* **2003**, *125*, 13541-13547.
- (5) He, L.; Musick, M. D.; Nicewarner, S. R.; Salinas, F. G.; Benkovic, S. J.; Natan, M. J.; Keating, C. D. *J. Am. Chem. Soc.* **2000**, *122*, 9071-9077.
- (6) Wang, J.; Xu, D.; Kawde, A.-N.; Polsky, R. *Anal. Chem.* **2001**, *73*, 5576-5581.
- (7) Zhang, J.; Song, S. P.; Wang, L. H.; Wu, H. P.; Pan, D.; Fan, C. H. *J. Am. Chem. Soc.* **2006**, *128*, 8575-8580.
- (8) Storhoff, J. J.; Marla, S. S.; Bao, P.; Hagenow, S.; Mehta, H.; Lucas, A.; Garimella, V.; Patno, T.; Buckingham, W.; Cork, W.; Muller, U. R. *Biosens. Bioelectron.* **2004**, *19*, 875-883.
- (9) Taton, T. A.; Mirkin, C. A.; Letsinger, R. L. *Science* **2000**, *289*, 1757-1760.

- (10) Cao, Y. W. C.; Jin, R.; Mirkin, C. A. *Science* **2002**, *297*, 1536–1540.
- (11) Park, S. J.; Taton, T. A.; Mirkin, C. A. *Science* **2002**, *295*, 1503–1506.
- (12) Wang, J.; Polsky, R.; Xu, D. *Langmuir* **2001**, *17*, 5739–5741.
- (13) Cai, H.; Xu, Y.; Zhu, N.; He, P.; Fang, Y. *Analyst* **2002**, *127*, 803–808.
- (14) Liu, C. H.; Li, Z. P.; Du, B. A.; Duan, X. R. *Anal. Chem.* **2006**, *78*, 3738–3744.
- (15) Ding, C. F.; Zhong, H.; Zhang, S. S. *Biosen. Bioelectro.* **2008**, *23*, 1314–1318.
- (16) Wang, J.; Liu, G.; Merkoci, A. *J. Am. Chem. Soc.* **2003**, *125*, 3214–3215.
- (17) Gerion, D.; Chen, F. Q.; Kannan, B.; Fu, A. H.; Parak, W. J.; Chen, D. J.; Majumdar, A.; Alivisatos, A. P. *Anal. Chem.* **2003**, *75*, 4766–4772.
- (18) Patolsky, F.; Lichtenstein, A.; Willner, I. *Angew. Chem. Int. Ed.* **2000**, *39*, 940–943.
- (19) Zhang, X. L.; Li, L. L.; Li, L.; Chen, J.; Zou, G. Z.; Si, Z. K.; Wen, R. J. *Anal. Chem.* **2009**, *81*, 1826–1832.
- (20) Wang, J.; Polsky, R.; Merkoci, A.; Turner, K. L. *Langmuir* **2003**, *19*, 989–991
- (21) Nam, J. M.; Stoeva, S. I.; Mirkin, C. A. *J. Am. Chem. Soc.* **2004**, *126*, 5932–5933.
- (22) Zhang, S. S.; Zhong, H.; Ding, C. F. *Anal. Chem.* **2008**, *80*, 7206–7212.